

SHING

CLOWASH

12

YCLOWASH

# The influence of swirl and turbulence anisotropy on CFD modelling for hydrocyclones

D M SMALL, A D FITT, and M T THEW  
University of Southampton, UK

## Abstract

In recent years, dewatering hydrocyclones have increased in importance as a cheap and efficient method for offshore bulk separation of oil and water. The reliability of such devices is compromised by the break-up of water droplets, resulting from high rates of shear within working hydrocyclones.

In the current study (carried out using the commercial code FLOW-3D) two specific questions are addressed:

(1) It is well known that CFD calculations in such circumstances are greatly influenced by choice of turbulence model. Because of the inherent anisotropy somewhat sophisticated models are required. How does the turbulence anisotropy increase with increasing swirl, and how can this be reflected in a realistic turbulence model?

(2) For commercial hydrocyclones, the inlet conditions are evidently not axisymmetric. Is it nevertheless possible to make accurate predictions using axisymmetric CFD models, or is it necessary to develop fully three-dimensional models?

These questions are discussed using a combination of theory and CFD calculations, and some conclusions are drawn regarding the viability of such procedures.

## 1 INTRODUCTION

The dewatering hydrocyclone offers considerable promise as a means for achieving the bulk separation offshore of oil and water. However, achieving the necessary reliability of such a device over the wide range of operating conditions met in the field has proved difficult. There are several causes of these difficulties:

- The viscosity of oil is higher than that of water, so that large centrifugal forces are needed to achieve separation in reasonable residence times.

- The viscosity ratio also makes water droplets vulnerable to break-up. This problem is exacerbated by the need for large swirl velocities, which promote high shear rates.
- The behaviour of the brine-in-oil dispersion near phase inversion (i.e. a change from oil continuous to brine continuous dispersion) is not well understood. In this regime effective viscosity of the mixture increases considerably.

The flow field inside a hydrocyclone is also complex, even with a single component of flow the anisotropic turbulence within the device makes accurate computational results difficult to obtain. However, a computational model of a de-watering hydrocyclone would be a valuable alternative to extensive experimental studies. The increasing maturity of the science of CFD, and the rapidly increasing capabilities of widely available computing hardware makes developing such a model an increasingly attractive possibility.

This paper seeks to investigate two important aspects of a computational model: Firstly turbulence modelling is considered, which reduces to a compromise between accuracy and computational cost. The  $k-\epsilon$  model, which assumes isotropy of turbulence, has been shown to be unsatisfactory for strongly swirling flows. In this paper a measure for turbulence isotropy is proposed, and used to show the increasing inadequacy of scalar eddy viscosity models with increasing swirl. The assumption of axisymmetry is examined. This assumption is always made in computational models of the hydrocyclone, on the grounds of computational economy. However, while this is a reasonable approach, it is necessary to consider carefully the boundary conditions for the model; in particular for the turbulent quantities.

## 1.1 Turbulence modelling

Many flows of engineering interest are turbulent, and in most of these cases it is not feasible to solve numerically the time-dependent Navier-Stokes equations with discretizations sufficiently fine to resolve the smallest scales of the turbulence. Even if this could be accomplished, the resulting computations would be of limited practical value. Efforts have therefore concentrated on producing a solution for the mean flow (after some averaging procedure has been applied) and a summary of the turbulent effects in an easily comprehensible form.

To achieve this, we begin with the unsteady Navier-Stokes equations,

$$\frac{\partial u_i}{\partial t} + u_j \frac{\partial u_i}{\partial x_j} = -\frac{1}{\rho} \frac{\partial p}{\partial x_i} + \nu \frac{\partial^2 u_i}{\partial x_j \partial x_j}, \quad (1)$$

$$\frac{\partial u_i}{\partial x_i} = 0, \quad (2)$$

where  $u_i$  denotes the velocity in the  $i$  direction,  $p$  denotes pressure, and  $\rho$  and  $\nu$  denote density and kinematic viscosity. The dependent variables of these equations  $u$  and  $p$  are subjected to the Reynolds' decomposition into mean and fluctuating components;  $u_i = U_i + u'_i$ ,  $p = P + p'$ , where capital letters denote the time-averaged components of the variables, and primes are attached to the unsteady components, whose time average is zero. Substituting these forms into equation 1, and taking the time-average of this system of equations yields

$$\frac{\partial U_i}{\partial t} + U_j \frac{\partial U_i}{\partial x_j} = -\frac{\partial P}{\partial x_i} - \frac{\partial \overline{u'_i u'_j}}{\partial x_j} - \nu \frac{\partial^2 U_i}{\partial x_j \partial x_j}, \quad (3)$$

where an overbar represents steady Navier-Stokes equations stress tensor  $-\overline{u'_i u'_j}$ .

In order to close this Reynolds' stresses in terms of the models used in engineering.

The Reynolds' stress equations also contain the link the two by some simple deviatoric stress tensor (postulated to be proportional

where  $S_{ij} = \frac{1}{2} \left( \frac{\partial u_i}{\partial x_j} + \frac{\partial u_j}{\partial x_i} \right)$  energy. The assumption as the Boussinesq eddy viscosity,  $\nu_t$ .

This method for production of models. These are known preferred direction on the flow straightforward to implement the fluid by a 'turbulent' are distinguished by their

This family of turbulence  $k-\omega$  model, the  $k-f$  model

The  $k-\epsilon$  model in particular simplicity, and reasonably

However, it is known confined swirling flows, Faced with this difficulty the  $k-\epsilon$  model, and have flows also.

Examples of this include viscosities were used in different viscosities be proportional  $k-\epsilon$  model is that one case which they have been used a modified equation for

However there are many in one form or another. It is desirable therefore turbulence models may

As the availability of increasingly becomes feasible

break-up. This problem promotes high shear rates.

transition (i.e. a change from laminar to turbulent). In this regime

with a single component of flow, the computational results for a swirling hydrocyclone would be of increasing maturity of the available computing facilities.

A compromise between accuracy and isotropy of turbulence, in this paper a measure of the inadequacy of scalar models for axisymmetry is examined. A reasonable approach, it is argued, is to use a model; in particular for

of these cases it is not possible to solve the equations with discretization. Even if this could be done, it has little practical value. Efforts to solve the equations in flow (after some averaging) to account for turbulent effects in an easily

equations,

(1)

(2)

where  $\rho$  and  $\nu$  denote the density and viscosity,  $u$  and  $p$  are the fluctuating components;  $\bar{u}$  and  $\bar{p}$  are the averaged components of the velocity and pressure, whose time average is denoted by a bar. The time-average of this system

(3)

$$\frac{\partial U_i}{\partial x_i} = 0, \quad (4)$$

where an overbar represents the time averaging operator. This system resembles the steady Navier-Stokes equations, except for the inclusion of the divergence of the Reynolds' stress tensor  $-\overline{u_i u_j}$ .

In order to close this system of equations it is necessary to propose a model for the Reynolds' stresses in terms of the mean flow quantities. This is the point of departure for the models used in engineering CFD calculations.

The Reynolds' stresses form a second rank tensor, and the averaged Navier-Stokes equations also contain the second rank mean stress tensor. It is natural to attempt to link the two by some simple relationship. It is customary to consider separately the deviatoric stress tensor (which has zero trace) from the pressure gradient; this is then postulated to be proportional to the deviatoric Reynolds' stress tensor. Thus

$$-\overline{u_i u_j} = \nu_T S_{ij} - \frac{2}{3} \delta_{ij} k, \quad (5)$$

where  $S_{ij} = \frac{1}{2} \left( \frac{\partial u_i}{\partial x_j} + \frac{\partial u_j}{\partial x_i} \right)$  is the mean stress tensor, and  $k = \frac{1}{2} \overline{u_i u_i}$  is turbulent kinetic energy. The assumption that the two stress tensors may be linked in this way is known as the Boussinesq eddy viscosity hypothesis. It is also necessary to postulate a form for the turbulent viscosity,  $\nu_T$ , in terms of the mean flow quantities.

This method for producing a model for the Reynolds' stress tensor is used by a family of models. These are known as isotropic turbulence models, since they impose no preferred direction on the flow other than that of the mean stress tensor. Such models are straightforward to implement; it is simply necessary to augment the laminar viscosity of the fluid by a 'turbulent viscosity' which varies throughout the flow field. Such models are distinguished by their method of determining such a viscosity.

This family of turbulence models includes the mixing length model,  $k-\epsilon$  model, the  $k-\omega$  model, the  $k-f$  models and many others.

The  $k-\epsilon$  model in particular is widely used in engineering CFD, as a result of its relative simplicity, and reasonable predictions in a wide variety of cases.

However, it is known (11),(6) that the  $k-\epsilon$  fails in some cases, particularly that of confined swirling flows, where the effects of the anisotropy of turbulence are important. Faced with this difficulty researchers have shown an understandable reluctance to reject the  $k-\epsilon$  model, and have attempted to modify it in such a way as to be suitable for these flows also.

Examples of this include (3), in which two separate (but proportional) turbulent viscosities were used in different directions, and (11), in which the requirement that the two viscosities be proportional was lifted. A disadvantage of such *ad hoc* modifications of the  $k-\epsilon$  model is that one cannot be sure of their validity outside the range of situations for which they have been tuned. Another method used to enhance the  $k-\epsilon$  method is to use a modified equation for  $\epsilon$ ; such models are described in (4) and (1).

However there are many situations (swirl burners, swirling jets) where the  $k-\epsilon$  model, in one form or another, is widely used, and gives good agreement with experimental data. It is desirable therefore to characterise quantitatively the regimes for which isotropic turbulence models may be used, and those where they are inapplicable.

As the availability of powerful computer hardware becomes more widespread, it increasingly becomes feasible to use more sophisticated turbulence models for the flows that

require them. The differential Reynolds' stress model (DRS) (7) is now included as an option in many commercial CFD codes. This model requires that a transport equation be solved for each independent component of the Reynolds' stress tensor, incorporating production, redistribution, diffusion and dissipation terms. Various sub-models have been proposed for these terms, creating a family of DRS models. In practice the models used in commercial CFD packages are fairly similar in structure (12). These additional equations must be solved as well as an equation for  $\epsilon$ ; this means solving 7 partial differential equations for turbulence effects, in addition to 4 for the mean flow quantities. The computational burden imposed by this method of modelling turbulence is significant, particularly since the coupling between the mean flow equations and the turbulent equations can no longer be achieved in terms of a turbulent viscosity.

In practice this leads to numerical instability of the resulting system of equations, and thus requires considerable relaxation of the numerical method. This in turn increases the computational effort involved in solving the equations.

## 2 MEASURING TURBULENCE ISOTROPY

### 2.1 Isotropy

In the laminar Navier-Stokes equations the kinematic viscosity,  $\nu$ , acts as an isotropic coefficient of diffusion. The class of turbulence models resulting from consideration of the time-averaged Navier-Stokes equations can be considered as defining more complex forms for the diffusion coefficient of momentum. The diffusion term arising in the averaged momentum equations (3) can then be written as

$$\frac{\partial}{\partial x_j} \left( \nu_{ik} \left( \frac{\partial U_k}{\partial x_j} + \frac{\partial U_j}{\partial x_k} \right) \right) \quad (6)$$

Isotropy of turbulence is thus defined in terms of the isotropy of the second rank tensor  $\nu$ . The most general form of a second rank isotropic tensor is

$$\nu_{ik} = A r_i r_k + B(r \delta_{ik}), \quad (7)$$

where  $r$  is the position vector. It is clear that the term proportional to  $r_i r_k$  is unphysical in a model for turbulent viscosity, and the remaining term is equivalent to prescribing an eddy viscosity. Thus a turbulent flow is isotropic precisely in so far as it can be predicted with an eddy viscosity model. Although the failure of such models in strongly swirling flows has been reported ((6), (11)) it is here sought to quantify the departure of the turbulence from isotropy, and to show the correlation between this behaviour and increasing swirl.

### 2.2 The Theory

In order to quantify the anisotropy of a turbulent flow field we must have some way of accurately predicting it. Measurements of second order velocity correlations which present sufficient detail for this purpose are not available for the strongly swirling flows investigated here. Accordingly CFD calculations using the DRS model have been used as a reference. This model, although not perfect, is widely accepted to be the most elaborate (and accurate) turbulence model typically available for engineering flows. In particular it

is the most complicated described here.

Denote the deviatoric stress tensor by  $\Sigma_{dij}$ . The

with some relation to turbulence; the turbulent

The above equation

where  $I$  is the identity tensor, the right hand side of such a method is used in equations only in terms of isotropy is

There are 6 constants (10) to be integrated as a result of the integrated form to

The equation (11) First the equation

The divergence of the surface integrals

where  $dA$  is taken over the surface. The equation is

where  $i$  ranges from 1 to 3

The stresses at cell centres.

Equation (14) and  $b$  the left hand

is the most complicated model built into the CFD package FLOW-3D, used in the work described here.

Denote the deviatoric mean stress tensor by  $S_{d ij}$ , and the deviatoric Reynolds' stress tensor by  $\Sigma_{d ij}$ . Then the hypothesis that we seek to test is that it is possible to write

$$\Sigma_{d ij} = \nu_T S_{d ij} \quad (8)$$

with some relationship for  $\nu_T$ . Equation 8 may be taken as a definition of isotropic turbulence; the turbulent effects have no preferred direction.

The above equation may be written

$$I \propto \Sigma_{d ij}^{-1} S_{d ij} \quad (9)$$

where  $I$  is the identity matrix, it is possible to develop a measure of the deviation of the right hand side of this equation from a multiple of the identity tensor. However, such a method is unsatisfactory. Both stress tensors enter into the averaged momentum equations only in terms of their divergence, so that the equation which must hold for isotropy is

$$\nabla \cdot \Sigma_{d ij} = S_{d ij} \cdot \nabla \nu_T + \nu_T \nabla \cdot S_{d ij} \quad (10)$$

There are 6 constants of integration involved in the transition from the differential form (10) to the integrated form (8). Although some constraints may be imposed between these constants as a result of the form of the eddy viscosity hypothesis, we may not expect the integrated form to hold exactly when using the DRS model.

The equation (10) must be manipulated before it can be used in a CFD calculation. First the equation is integrated over a control volume  $V$  to give

$$\int_V \nabla \cdot \Sigma_{d ij} dV = \int_V S_{d ij} \cdot \nabla \nu_T dV + \nu_T \int_V \nabla \cdot S_{d ij} dV \quad (11)$$

The divergence theorem may then be used to transform two of the volume integrals to surface integrals:

$$\int_S \Sigma_{d ij} \cdot dA = \int_V S_{d ij} \cdot \nabla \nu_T dV + \int_S S_{d ij} \cdot dA, \quad (12)$$

where  $dA$  is taken to be an outward normal to the cell.

The equation discretizes in a straightforward manner.

$$\sum_i \Sigma_{d ij} \cdot A_i = V S_{d ij} \cdot \nabla \nu_T + \nu_T \sum_i S_{d ij} \cdot A_i \quad (13)$$

where  $i$  ranges over the faces of the cell. Or,

$$\sum_i \Sigma_{d ij} \cdot A_i - V S_{d ij} \cdot \nabla \nu_T \propto \sum_i S_{d ij} \cdot A_i \quad (14)$$

The stresses at cell faces are evaluated by means of linear interpolation from neighbouring cell centres.

Equation (14) allows a straightforward parametrization of isotropy; denoting by  $a$  and  $b$  the left and right hand expressions of (14) we define an isotropy parameter,  $\eta$ , by

$$\eta = \frac{a \cdot b}{|a| |b|} \quad (15)$$

## 2.3 The Simulations

A series of simulations of the flow in a conventional hydrocyclone was performed, based on a geometry (hydrocyclone number 1) described in (9). This hydrocyclone has diameter 75mm, and a total cone angle of 20°. One deviation from the circumstances assumed in (9) was that the cyclone was assumed to be operating without an air core. This was partly a result of a desire not to complicate the model unduly, and also a reflection of the status of this work as a preliminary to the authors' work on liquid-liquid hydrocyclones operating without gas-cores. It is not felt that this departure will have too deleterious an effect on the model's worth as an indicator of the usefulness of the various turbulence models considered.

A series of simulations was performed using this geometry with varying swirl, using the commercial CFD code FLOW-3D. The degree of swirl was characterised in the first instance by the inlet swirl angle, a parameter which requires some explanation. In the axisymmetric simulation a section of the side wall of the hydrocyclone is designated as an inlet. In FLOW-3D it is necessary for the flow at an inlet to have a component of velocity perpendicular to the inlet, in order for the flow to enter the solution domain. The radial velocity was thus fixed for all the simulations in order to give a flow-rate of 67 kg/min (1.12 m<sup>3</sup>/s), as used in (9). The azimuthal inlet velocity may then be adjusted arbitrarily, without affecting the volume flux through the device. The inlet angle,  $\alpha$  is then defined to be  $\arctan(v_\theta/v_r)$ .

Although this parameter may be used to characterize the intensity of the swirl before the simulation is carried out, afterwards the swirl number, which seeks to measure the ratio of the axial flux of axial momentum to the axial flux of azimuthal momentum,

$$S = \frac{\int_0^{R_{wall}} V_\theta |V_z| r^2 dr}{R_{wall} \int_0^{R_{wall}} V_z^2 r dr}, \quad (16)$$

may be calculated. This is one popular definition of swirl number (8), several other definitions exist of similar parameters. An additional post-processing was the calculation of the split ratio, 1-F, where F is the ratio of volumetric flux through the underflow to the total volumetric flux through the device.

The calculations were performed using a grid with 15 subdivisions radially, and 40 axially on the cyclone body. Extended outlets were used in order to mitigate the effects of the downstream boundary conditions, which were of zero gradient type. The solution method used was the finite volume method, as described in (10), using the hybrid differencing scheme. Attempts to use higher order schemes resulted in numerical instabilities.

Each of the simulations took of the order of 3 hours of CPU time on a Sun Centre 1000 computers. This is largely a result of the need for considerable numerical under-relaxation during the solution of the discretized equations; attempts to accelerate convergence usually lead instead to divergence of the numerical method. Given the high computational cost of the solution method, it is understandably desirable to use more economical turbulence models where possible.

Table (1) tabulates the split ratios, pressure drops and swirl numbers for each of the simulations.

Swirl Ang $\alpha$ (°)
10
20
30
50
70
80

Table

Figures 1,2,3,4,5 show for low values of the inlet swirl angle which decreases in size of inwardly directed flow responsible for the region

For the 50 degree inlet swirl angle it is expected in an operating hydrocyclone equation 15 within the hydrocyclone. For a degree of swirl it becomes more effective in reducing the value of  $\eta$  is found to be no correlation between  $\eta$  and swirl angle.

Throughout all the simulations the flow is approximately solid body

## 3 THREE D

### 3.1 Introduction

Most computational models are axisymmetric, and solid body rotation. There is no reason to suppose that boundary conditions of a hydrocyclone mean expansion.

In an axisymmetric simulation the side wall of the device, the boundary conditions imposed for the turbulence models are seriously underestimated. The values of  $\eta$  represent the values of  $\eta$  in the region near the inlet.

This is particularly true for the effects of turbulent shear in the region near the inlet.

one was performed, based hydrocyclone has diameter circumstances assumed in out an air core. This was and also a reflection of the liquid-liquid hydrocyclones will have too deleterious s of the various turbulence

with varying swirl, using s characterised in the first some explanation. In the cyclone is designated as an ve a component of velocity lution domain. The radial e a flow-rate of 67 kg/min en be adjusted arbitrarily, et angle,  $\alpha$  is then defined

intensity of the swirl before hich seeks to measure the zimuthal momentum,

$$(16)$$

ber (8), several other def- essing was the calcluation through the underflow to

sions radially, and 40 axi- o mitigate the effects of the ype. The solution method ng the hybrid differencing erical instabilities.

time on a Sun Centre 1000 numerical under-relaxation elerate convergence usually e high computational cost ore economical turbulence

rl numbers for each of the

Swirl Angle $\alpha$ (°)	Pressure Drop $\Delta P$ (Pa)	Split Ratio 1-F	Swirl Number S
10	$4.19 \times 10^3$	0.776	0.024
20	$4.33 \times 10^3$	0.776	0.048
30	$4.78 \times 10^3$	0.783	0.079
50	$6.27 \times 10^3$	0.792	0.149
70	$1.16 \times 10^4$	0.842	0.160
80	$1.97 \times 10^4$	0.896	0.391

Table 1: Summary of Computational Results

Figures 1,2,3,4,5 show that the turbulence throughout most of the flow field is isotropic for low values of the inlet angle. Also at low swirl values, there is a region of anisotropy which decreases in size with increasing swirl. For low swirl the entry flow forms a ring of inwardly directed fluid. It seems reasonable that the collisions of this ring of fluid are responsible for the region of anisotropy.

For the 50 degree inlet angle case, which is still a much lower swirl than would be expected in an operating hydrocyclone, the value of the isotropy parameter,  $\eta$  defined by equation 15 within the cyclone body lies mostly within the 0.27 to 0.48 band. At this degree of swirl it becomes difficult to believe that the  $k-\epsilon$  model, which assumes  $\eta = 1$  could be effective in reproducing the flow field. As swirl is increased further, it is seen that the value of  $\eta$  is further reduced, until at an 80 degree swirl angle, there is effectively no correlation between the directions of the mean and turbulent stresses in much of the cyclone.

Throughout all these simulations the flow near the axis, which is characterized by approximately solid body rotation, remains a region of relatively high isotropy.

### 3 THREE DIMENSIONAL MODELLING

#### 3.1 Introduction

Most computational models of hydrocyclones make the assumption that the flow field is axisymmetric, and solve for the flow only on a cross-section of the device. While there is no reason to suppose this procedure is invalid, it requires careful attention to the boundary conditions specified at the inlet. In practice, the single or twin tangential inlets of a hydrocyclone mean that the flow comes into the cyclone chamber by way of a sudden expansion.

In an axisymmetric model of a hydrocyclone, where the inlet is modeled as a ring on the wall of the device, the effects of the expansion are not modeled. If the boundary conditions imposed for the turbulent quantities  $k$  and  $\epsilon$  then there exists the possibility that these are seriously underestimated; the boundary conditions for an axisymmetric model must represent the values of any turbulent quantities just within the cyclone chamber.

This is particularly important in the case of liquid-liquid hydrocyclones, since the effects of turbulent shear at the inlet may have an important effect on droplet break-up in the region near the inlet. This in turn has an important effect on separation performance.

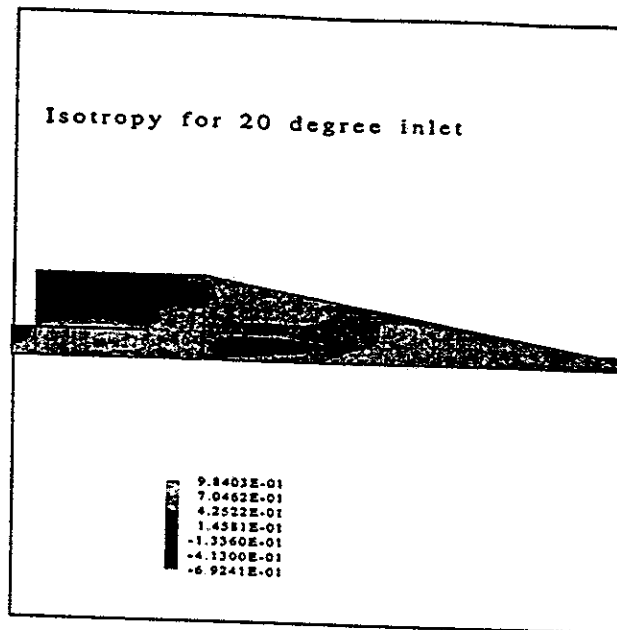


Figure 1: Isotropy for 20° inlet angle

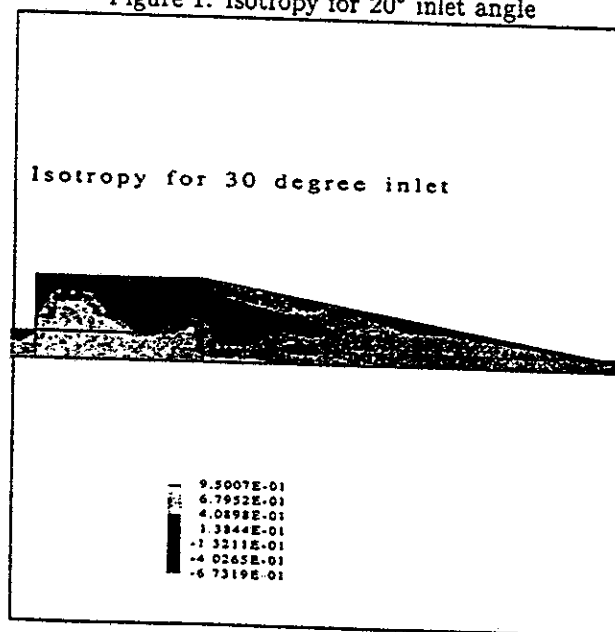


Figure 2: Isotropy for 30° inlet angle

### 3.2 The Simulation

The computational expense of a fully three dimensional model of a hydrocyclone is prohibitive. However, it is possible to use a much simplified three-dimensional model of the inlet region as a guide to setting realistic conditions for an axisymmetric model. Accordingly a model was developed in which the cyclone chamber was represented by a cylinder

(75mm in diameter),  
 ameter). This was m  
 the inlet pipes were t



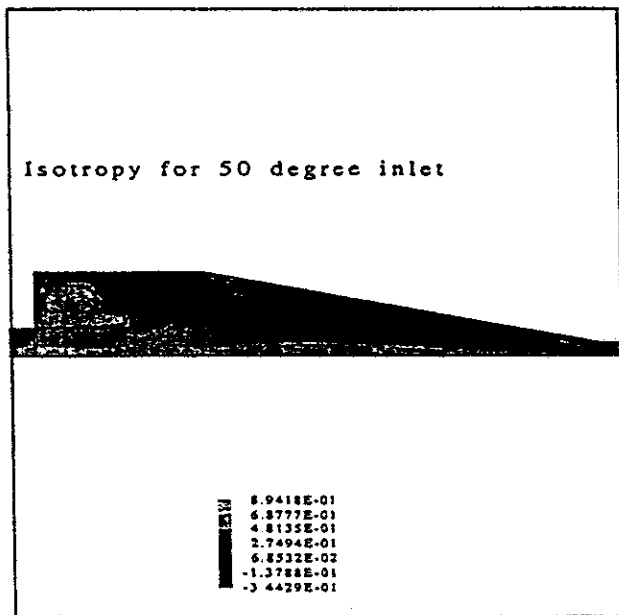


Figure 3: Isotropy for 50° inlet angle

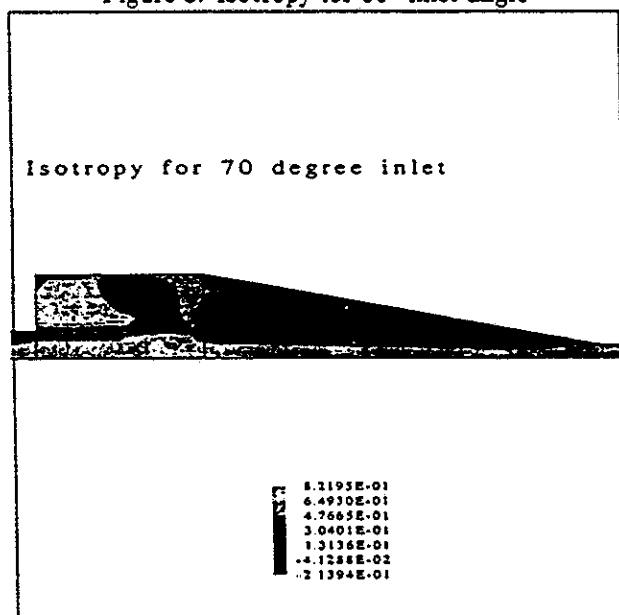


Figure 4: Isotropy for 70° inlet angle

of a hydrocyclone is pro-  
 -dimensional model of the  
 symmetric model. Accord-  
 : represented by a cylinder

(75mm in diameter), with two tangential inlets of cylindrical cross-section (25mm in diameter). This was modeled using FLOW-3D. The turbulent boundary conditions inside the inlet pipes were taken to be those deduced from fully developed pipe flow (2):

$$k_{inl} = C_{p1} |U_{inl}|^2 \quad (17)$$

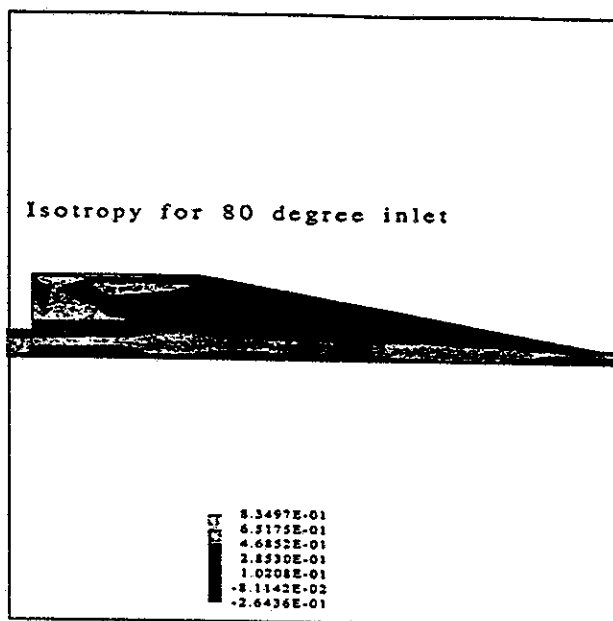


Figure 5: Isotropy for 80° inlet angle

$$\epsilon_{inl} = \frac{k_{inl}}{C_{p2}} D \quad (18)$$

where  $C_{p1} = 0.002$  and  $C_{p2} = 0.3$  are empirical constants, and  $D$  is the inlet diameter. The turbulence model used was the DRS model.

The geometry was modeled using 96 subdivisions axially, and a 16 by 16 body-fitted grid across the circular cross-section of the cyclone body. The cyclone body was extended axially sufficiently far, it is hoped, that the downstream zero-gradient boundary conditions should have little impact on flow quantities near the inlet region. In any case, the size of this simulation made it difficult to accommodate on a shared computer. The simulation took approximately 3 hours of CPU time, on a SUN Centre 1000 computer, for 500 iterations of the outer loop of the SIMPLEX procedure described in (10). Surprisingly, this number of iterations was sufficient to obtain adequate convergence, and the model was much less prone to numerical instabilities than in the axisymmetric case. However, the computational burden of this simulation makes it clear that three dimensional models are still unsuited for investigating realistic hydrocyclone geometries.

### 3.3 Discussion of results

The results, as presented in Figures 6 and 7, show peaks in turbulent intensity just beyond the junction of the inlets and the cyclone body. This is to be expected; the flow at the inlets can be thought of as driving the flow within the hydrocyclone, and significant shear would be anticipated in this region. The peaks in the values of  $\epsilon$  are particularly significant; with a peak intensity four orders of magnitude above the typical value elsewhere in the cyclone body. It may be that the computational model exaggerates the height of these peaks, but, even so, the effect of such localised peaks in turbulence intensity is likely to

Figure

have a profound effect  
It is clear from the  
axisymmetric simulation  
design used in this model  
those used for liquid-l  
stration of the turbule



(18)

$D$  is the inlet diameter.

and a 16 by 16 body-fitted cyclone body was extended to meet periodic boundary conditions. In any case, the size of the computer. The simulation was run on a 1000 computer, for 500 iterations. Surprisingly, convergence, and the model was symmetric case. However, the three dimensional models were tried.

turbulence intensity just beyond the inlet; the flow at the inlets and significant shear would be particularly significant; the calculated value elsewhere in the cyclone generates the height of these turbulence intensity is likely to

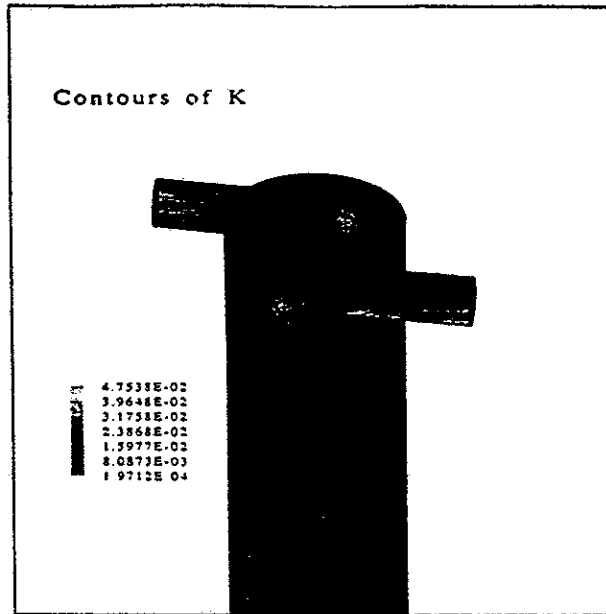


Figure 6: Turbulent Kinetic Energy

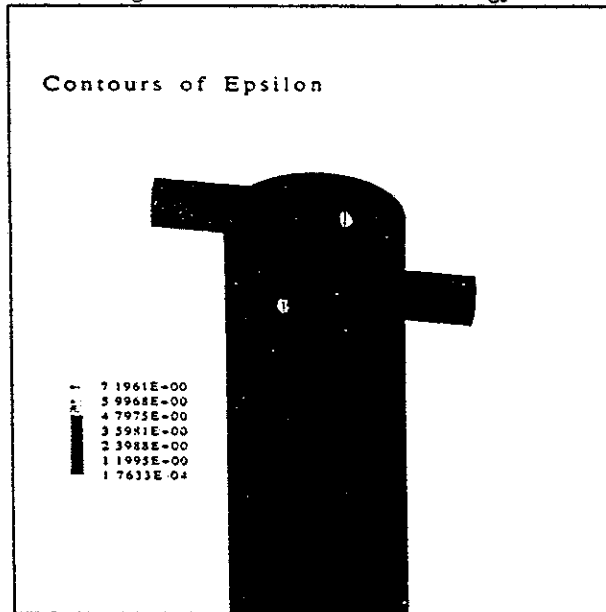


Figure 7: Rate of Dissipation of Turbulence Kinetic Energy

have a profound effect on liquid-liquid separation.

It is clear from these results that the standard inlet conditions for  $k$  and  $\epsilon$  in axisymmetric simulations represent considerable underestimates. However, the simple inlet design used in this model - chosen for modelling convenience - is not representative of those used for liquid-liquid separation. Although this case is quite extreme in its demonstration of the turbulence peaks, the phenomenon demonstrated is likely to be significant

in hydrocyclones with more carefully designed inlets. To discover the extent of this phenomenon in such cases will require further work.

## 4 CONCLUSIONS

A method for quantifying turbulence anisotropy has been presented, and used to investigate the validity of eddy viscosity models of turbulence, using a DRS model as a reference. The results show that for moderate swirl (swirl numbers of 0.1 or higher) the  $k-\epsilon$  model is unsuitable and must be replaced by a model capable of reproducing anisotropic turbulence effects. It is interesting to note that the algebraic stress model, as implemented in FLOW-3D, although in theory capable of reproducing anisotropic flow fields, has proved impossible to converge in strongly swirling flows; a difficulty acknowledged by AEA Technology (5), the authors of the code.

Three dimensional simulations of the inlet region have shown that this region contains zones of high turbulence intensity, whose effect on droplet breakup is likely to be significant. While these results do not preclude the use of axisymmetric models for liquid-liquid hydrocyclones, they suggest that the boundary conditions for inlet turbulence must be reconsidered.

### 4.0.1 Acknowledgements

One of the authors (D.S.) acknowledges the financial support of the Marine Technology Directorate during this work.

## References

- (1) E G Hauptmann A Malhotra, R M R Branion. Modeling the flow in a hydrocyclone. *Canadian Journal of Chemical Engineering*, 72:953-960, 1994.
- (2) AEA Technology, Computational Fluid Dynamics Services, Building 8.19, Harwell Laboratory, Oxfordshire, UK. *CFDS-FLOW3D User Guide*, 1994.
- (3) F Boysan, R Weber, J Swithenbank, and P A Roberts. Modeling coal-fired cyclone combustors. *Combustion and Flame*, 63:73-86, 1986.
- (4) H F Boysan. Renormalization group theory based turbulence models and their applications to industrial problems. In *Engineering Applications of Computational Fluid Dynamics*, pages 43-47, 1993.
- (5) AEA Technology D Burt. Private communication. 1995.
- (6) J.H.Hargreaves and R.S. Silvester. Computational fluid dynamics applied to the analysis of deoiling hydrocyclone performance. *Trans IChemE*, 68:365-383, 1990.
- (7) B E Launder, G J Reece, and W Rodi. Progress in the development of a Reynolds' stress turbulence closure. *J. Fluid Mech.*, 68:537-566, 1975.
- (8) A Loader. *Instability and turbulence in confined swirling flow investigated by laser doppler anemometry*. PhD thesis, University of Southampton, 1981.

(9) T C Monredon, K an investigation c 35:65-83, 1992.

(10) S.V. Patankar. *N*

(11) R.K.Duggins and editor, *Third BH*.

(12) H K Versteeg an *Volume Method*.

r the extent of this phe-

ed, and used to investi-  
RS model as a reference.  
or higher) the  $k-\epsilon$  model  
ncing anisotropic turbu-  
odel, as implemented in  
ic flow fields, has proved  
owledged by AEA Tech-

that this region contains  
up is likely to be signifi-  
: models for liquid-liquid  
alet turbulence must be

the Marine Technology

e flow in a hydrocyclone.  
94.

, Building 8.19, Harwell  
, 1994.

deling coal-fired cyclone

ilence models and their  
*ations of Computational*

ynamics applied to the  
*E*, 68:365-383, 1990.

elopment of a Reynolds'

low investigated by laser  
on, 1981.

- (9) T C Monredon, K T Hsieh, and R K Rajamani. Fluid flow model of the hydrocyclone: an investigation of device dimensions. *International Journal of Mineral Processing*, 35:65-83, 1992.
- (10) S.V. Patankar. *Numerical Heat Transfer and Fluid Flow*. Hemisphere Books, 1980.
- (11) R.K.Duggins and P.C.W.Frith. Turbulence effects in hydrocyclones. In P. Wood, editor, *Third BHRA Conference on Hydrocyclones*, pages 75-82, 1987.
- (12) H K Versteeg and W Malalasekera. *Computational Fluid Dynamics, The Finite Volume Method*. Longman Scientific and Technical, 1995.